Available online at www.sciencedirect.com
ScienceDirect
Journal of Sound and Vibration 322 (2009) 674–689
JOURNAL OF SOUND AND VIBRATION
www.elsevier.com/locate/jsvi

Predicting the effect of temperature on the performance of elastomer-based rail damping devices

N. Ahmad[a], D.J. Thompson[a,*], C.J.C. Jones[a], A.H. Muhr[b,1]

[a]*Institute of Sound and Vibration Research, Highfield, Southampton SO17 1BJ, UK*
[b]*Tun Abdul Razak Research Centre, Brickendonbury, Hertford SG13 8NL, UK*

Received 26 March 2008; received in revised form 14 November 2008; accepted 17 November 2008
Handling Editor: C.L. Morfey
Available online 8 January 2009

Abstract

Damping devices for railway tracks have been developed in recent years in which a tuned mass-spring absorber system is formed by an elastomeric material and embedded steel masses. The loss factor and stiffness of the elastomer are very important for the performance of the system but, unfortunately, both properties are sensitive to changes in the temperature. Although having a high loss factor gives good noise reduction, it also means greater variation of stiffness, and consequently tuning frequency, with temperature. Conversely, with lower loss factors the tuning frequency can be kept close to the target but a smaller noise reduction is achieved.

To investigate the effect of the temperature on the performance of a generic rail absorber, a simple Timoshenko beam model of the track is used. To this is added a single-frequency continuous tuned absorber. The noise reduction at each frequency is estimated from the ratio of the track decay rates of treated and untreated rails.

There is a physical link between the damping loss factor and the stiffness variation with temperature, of which account must be taken. The rate of change of stiffness with log frequency is established by assuming a constant value of loss factor. Using the time-temperature superposition principle, this is expressed in terms of temperature dependence. This is used in the prediction of decay rates and thereby noise reduction at different temperatures. This leads to an assessment of the relative importance of using a high damping loss factor or a temperature-independent stiffness.

Finally, a method of weighting the noise reduction at different temperatures is investigated. A distribution of rail temperatures at a site in the UK is used to develop a weighting procedure. This is extended to account for temperature variations at other locations, where less data are available.

1. Introduction

The major source of noise from railway vehicles is wheel–rail rolling noise. This broadband noise is caused by the vibrations of the wheels, rails and sleepers induced by the irregularities (roughness) on the surface of the wheel and rail [1]. The wheel is usually the dominant source of noise at high frequency, typically above about

*Corresponding author. Tel.: +44 2380592294; fax: +44 2380593190.
E-mail address: djt@isvr.soton.ac.uk (D.J. Thompson).
[1]Tel.: +44 1992584966; fax: +44 1992554837.

0022-460X/$ - see front matter © 2008 Elsevier Ltd. All rights reserved.
doi:10.1016/j.jsv.2008.11.031

2 kHz. The sleeper can become the dominant source below 400 Hz. However, the rail is usually the greatest source in the frequency range 500–2000 Hz and often forms the most important contribution overall [2]. Several methods are available to reduce rolling noise; in particular noise barriers can be used but these are expensive and have other disadvantages. Moreover, various studies have shown that noise control at source is generally more cost-effective than using barriers [3]. One method of control at source that has been shown to be effective is to use rail dampers (or 'absorbers') on the track. In one application a reduction of 6 dB(A) was found in the rail component of noise [4].

This paper considers an important aspect in the optimisation of the design of a rail absorber. The class of absorbers considered here, as in Ref. [4], is based on an elastomeric material which is used with steel masses to form a tuned mass-spring system. The stiffness and loss factor of the elastomer are very important for the performance of such a system but both properties are sensitive to changes in the temperature. This must be taken into account as the device is required to operate in a range of environmental temperatures between about -20 and 40 °C. Ideally, the elastomer in such a rail absorber should have a relatively high loss factor and a stiffness which does not vary strongly with temperature but these are physically conflicting requirements [5]. The key question is how to reach a suitable compromise between these two requirements.

In order to demonstrate a suitable methodology, a simple model of a generic vibration absorber attached to a railway track is introduced and used to study the influence of the stiffness and damping of the elastomer on the noise reduction. A physically-consistent estimate is made of the frequency-dependence of the stiffness by assuming a constant loss factor. Then, by using the time–temperature superposition principle, this is expressed as a temperature-dependence of the stiffness. This is used to estimate the noise reduction as a function of temperature. The aim is to determine the relative merits of high damping or a low variation in stiffness, in order to establish a practical target for a new material.

Although the assumption of a constant loss factor represents a gross simplification of the behaviour of real materials, it enables trends to be established without using the properties of any particular material. These general trends allow insight to be gained into the inter-dependence of the temperature-dependence of stiffness and the amount of damping. The method can also be used with the stiffness and damping properties of real materials but this is beyond the scope of the present paper.

It should also be pointed out that the radiation of noise from the absorber mass itself can be an issue for lightly damped absorbers, although in Ref. [4] it was found to contribute less than 1 dB to the rail noise for a practical case. However, this is considered to be a secondary effect and in the present analysis this additional noise radiation is neglected.

The rail temperature varies considerably in the course of a year, affecting the performance of the rail absorber. The statistical distribution of rail temperatures is, therefore, investigated and used to develop a weighting procedure with which to account for temperature variation. A method is presented from which plausible rail temperature distributions can be derived from the daily maximum and minimum air temperature data, which is the form of data most commonly available. Temperature distributions for the UK, Sweden and Italy are evaluated. The results obtained provide weighting functions for the noise reduction. This method can be used to assess various elastomeric materials to determine the optimum material for a given situation in terms of the average noise reduction.

2. Model for track vibration and decay rate

The noise from the track depends on the rate of decay of waves propagating along the rail [6]. The sound power radiated by the rail is proportional to $1/\Delta$, where Δ is the decay rate in dB/m. This is given by

$$\Delta = -8.686\ \mathrm{Im}(k) \tag{1}$$

where k is the complex wavenumber of waves in a rail [7].

An initial study is presented in this section using a simple track model to identify the effect of varying these parameters. The untreated track is modelled as a beam on a damped elastic foundation (rail pad), as shown in Fig. 1(a). By introducing the damped mass-spring system (absorber), as shown in Fig. 1(b), an estimate is obtained for the decay rate of the track with a generic absorber. The ratio of the decay rates of the treated and untreated rails is used to determine the effect of the damping device.

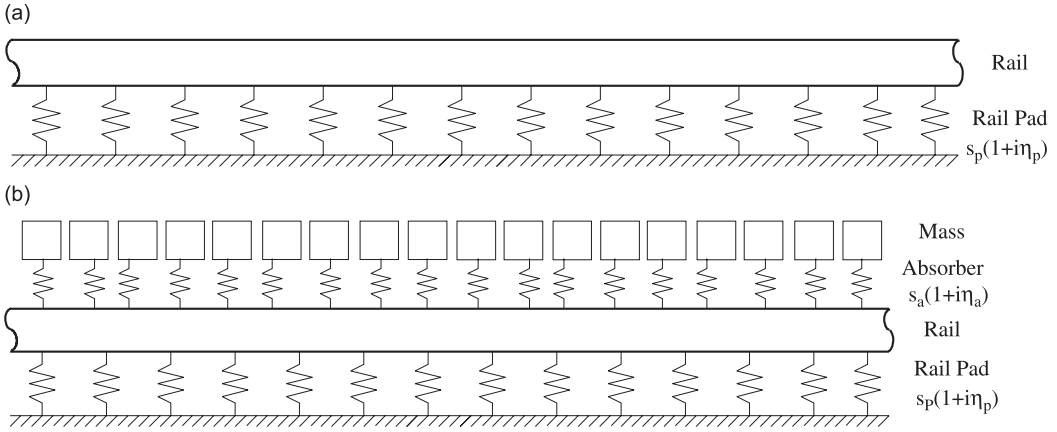

Fig. 1. Schematic diagram of (a) untreated track and (b) treated track.

The track is modelled as a Timoshenko beam (see e.g. Refs. [8,9]) on an elastic layer of stiffness s_p per unit length. The equations of motion are

$$GA\kappa\frac{\partial}{\partial x}\left(\phi-\frac{\partial u}{\partial x}\right)+s_p u+\rho A\frac{\partial^2 u}{\partial t^2}=F\delta(x)e^{i\omega t} \tag{2}$$

$$GA\kappa\left(\phi-\frac{\partial u}{\partial x}\right)-EI\frac{\partial^2\phi}{\partial x^2}+\rho I\frac{\partial^2\phi}{\partial t^2}=0 \tag{3}$$

where u is the vertical deflection, ϕ is the rotation of the cross-section relative to the undeformed axis, κ is the shear coefficient, $\kappa<1$, ρ is the density, A is the cross-sectional area, I is the second moment of area, E is Young's modulus and G is the shear modulus.

To find the dispersion relation free wave solutions are sought of the form $u(x,t)=Ue^{ikx}e^{i\omega t}$ and $\phi(x,t)=U\Psi e^{ikx}e^{i\omega t}$, where U is the complex amplitude of u and $U\Psi$ is the corresponding amplitude of ϕ. From Eq. (3) Ψ is given by

$$\Psi=\frac{-ikGA\kappa}{\rho I\omega^2-GA\kappa-EIk^2} \tag{4}$$

The dispersion relation can be obtained by substituting this equation into Eq. (2) giving

$$k^4+C_2(\omega)k^2+C_3(\omega)=0 \tag{5}$$

where

$$C_2(\omega)=\left(\frac{s_p-\rho A\omega^2}{GA\kappa}\right)-\left(\frac{\rho I\omega^2}{EI}\right) \tag{6}$$

$$C_3(\omega)=\left(\frac{s_p-\rho A\omega^2}{EI}\right)\left(1-\frac{\rho I\omega^2}{GA\kappa}\right) \tag{7}$$

Damping can be introduced by making E, G and s_p complex with the form $E(1+i\eta_r)$, $G(1+i\eta_r)$ and $s_p(1+i\eta_p)$, where η_r is the loss factor of the rail and η_p is the loss factor of the rail pad.

For the treated track, a similar procedure is followed except that the absorber is introduced onto the existing beam as shown in Fig. 1(b). Its dynamic stiffness is

$$s_{\mathrm{dyn}}(\omega)=\left(\frac{1}{s_a}-\frac{1}{\mu_a\omega^2}\right)^{-1}=s_a-\frac{s_a^2}{s_a-\mu_a\omega^2} \tag{8}$$

where μ_a is the mass of the absorber per unit length of rail and s_a is the absorber stiffness per unit length. As before, this can be made complex with the form $s_a(1+i\eta_a)$, where η_a is the loss factor of the absorber material.

The stiffness can be chosen according to the 'tuning' frequency of the absorber, which is obtained from $\omega_a = \sqrt{s_a/\mu_a}$. s_{dyn} should be added to s_p, giving a modified value of C_2 and C_3.

Fig. 2 shows the predicted decay rate obtained from this model, using the parameters listed in Table 1. The decay rate of the untreated track shows a similar trend to measured ones (see e.g. Ref. [4]). Although the sleepers and ballast are omitted from this model, these have little effect on the decay rate at frequencies above about 400 Hz, where propagating waves occur in the rail. This frequency corresponds to the drop in decay rate seen in Fig. 2. A rail absorber only has effect above this frequency [7].

In the track model, damping is added to the rail to ensure that the predictions follow the trend of measured curves, especially above 1 kHz. Otherwise, the curve would continue to fall at high frequency [7]. However, it is known that in practice this damping is not associated with the rail itself, but with the rail pad, the damping effect of which is increased at high frequencies due to cross-sectional deformation of the rail.

Fig. 2 also shows the decay rate of the treated track for the parameters given in Table 1. The tuning frequency of the absorber is set to 1000 Hz. The absorber introduces a large peak in the decay rate between 500 and 3000 Hz with its maximum around the tuning frequency. This corresponds to the region where the rail

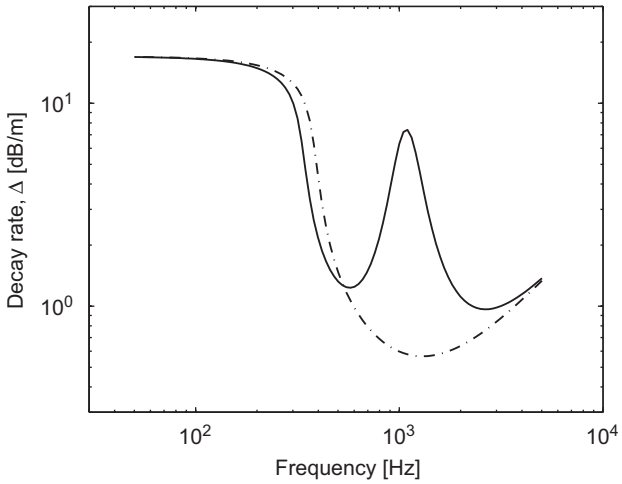

Fig. 2. The decay rate of the untreated (– · –) and treated (—) track. The parameters used are listed in Table 1.

Table 1
Parameters used for railway track including absorber.

Rail		
Cross-sectional area	A	$7.68 \times 10^{-3}\,\mathrm{m}^2$
Second moment of area	I	$3.0 \times 10^{-5}\,\mathrm{m}^4$
Young's modulus for steel	E	$2.11 \times 10^{11}\,\mathrm{N/m}^2$
Density for steel	ρ	$7850\,\mathrm{kg/m}^3$
Timoshenko shear coefficient for rail	κ	0.4
Poisson's ratio	ν	0.3
Damping loss factor of rail	η_r	0.02
Pad		
Support stiffness per unit length	s_p	$3.80 \times 10^8\,\mathrm{N/m}^2$
Damping loss factor of support	η_p	0.16
Absorber (default values)		
Stiffness per unit length	s_a	$6.91 \times 10^8\,\mathrm{N/m}^2$
Mass per unit length	m_a	17.5 kg/m
Damping loss factor	η_a	0.35

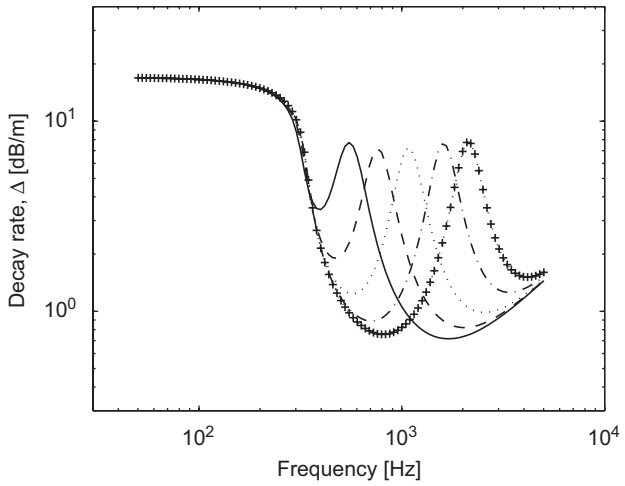

Fig. 3. The decay rate of the rail with absorber for various values of absorber stiffness. —, $s_a = 1.73 \times 10^8\,\mathrm{N/m^2}$ (500 Hz); − − −, $s_a = 3.39 \times 10^8\,\mathrm{N/m^2}$ (700 Hz); ···, $s_a = 6.91 \times 10^8\,\mathrm{N/m^2}$ (1000 Hz); − · −, $s_a = 15.5 \times 10^8\,\mathrm{N/m^2}$ (1500 Hz); +, $s_a = 27.6 \times 10^8\,\mathrm{N/m^2}$ (2000 Hz).

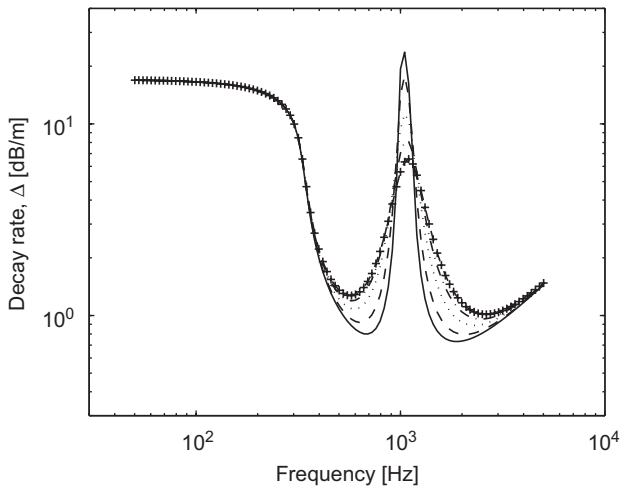

Fig. 4. The decay rate of the rail with absorber for various absorber loss factors: —, $\eta_a = 0.05$; − − −, $\eta_a = 0.1$; ···, $\eta_a = 0.2$; − · −, $\eta_a = 0.4$; +, $\eta_a = 0.8$.

noise component is dominant (see Section 3). The added mass of the absorber slightly reduces the cut-on frequency of propagating waves in the rail and, hence, reduces the decay rate between 200 and 500 Hz [7].

Fig. 3 shows the effect of increasing the stiffness of the absorber. This increases its tuning frequency. Fig. 4 shows that increasing the loss factor of the absorber will increase the breadth but decrease the peak of the decay rate. For high loss factors, the peak of the decay rate is also shifted slightly towards higher frequencies. In order to determine the relative merits of the breadth and height of this peak, these results must be combined with noise predictions; these are considered in the next section.

3. Predicted rail noise

In order to estimate the effect on the radiated sound, a prediction is made of the sound power radiated from an untreated track using the TWINS model [10]. The sound power of the damped track is then calculated by

modifying the rail noise component predicted by the TWINS model in accordance with the ratio of decay rates.

Fig. 5 shows the initial sound power spectrum predicted using TWINS. The separate components radiated by the wheel, rail and sleeper are shown. This initial situation represents a typical modern track with relatively soft rail pads, as in Section 2, a train speed of 100 km/h and a roughness spectrum corresponding to wheels with cast-iron block tread brakes.

The noise from the rail is composed of components due to both vertical and lateral vibration. In this untreated situation the vertical component is 7.5 dB greater than the lateral component. Even in the treated situation, if the vertical component is modified by the effect of the rail absorbers but the lateral component is left unaffected, the vertical component would still be greater than the lateral component. In practice, the absorbers will also introduce some damping to lateral vibration. However, from these comparisons it can be concluded that the lateral component can be neglected in optimising the effect of the absorber because of the dominance of the vertical motion.

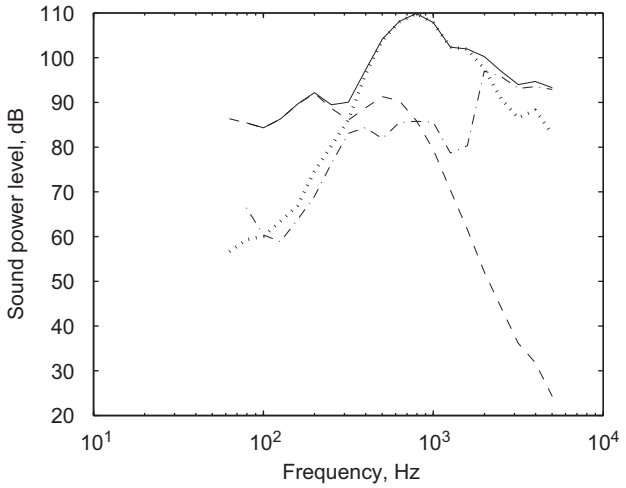

Fig. 5. The initial sound power level from one wheel and associated track predicted using TWINS. —, total; – · –, wheel; · · ·, rail; – – –, sleeper.

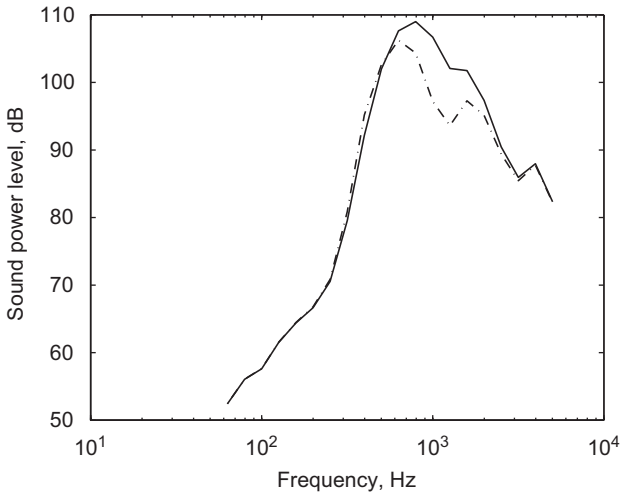

Fig. 6. The predicted vertical component of rail noise with and without absorber. The input parameters are as in Table 1, tuning frequency 1000 Hz, $\eta_a = 0.35$. —, vertical untreated (113.2 dB(A)); – – –, vertical treated track (109.1 dB(A)).

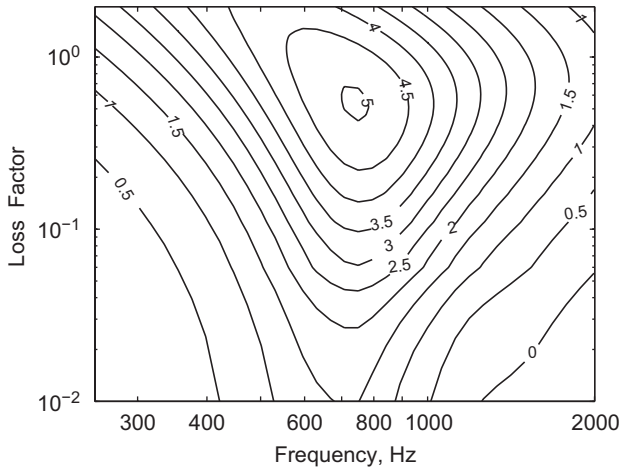

Fig. 7. Contour plot of reduction of rail vertical component of noise in dB(A) for a range of loss factor and stiffness (corresponding to tuning frequency between 250 and 2000 Hz).

The predicted noise reduction has, therefore, been calculated in terms of the reduction in the vertical component. The sound power levels of treated and untreated tracks are shown in Fig. 6. These are obtained using the parameters given in Table 1. The absorber is found to give an overall reduction of 4.1 dB(A) in this component of rail noise. The maximum effect is about 10 dB occurring in the 1000 Hz band; this can also be seen from the ratio of the decay rates in Fig. 2. Note that the vertical component of rail vibration consists of a propagating wave and a nearfield wave; only the decay rate of the propagating wave is modified in this calculation.

Fig. 7 shows the reduction in overall A-weighted noise from the rail vertical motion found for a range of values of the loss factor and stiffness (corresponding to a range of tuning frequency of 250–2000 Hz). This shows that the maximum noise reduction is achieved for loss factors of 0.3 and above, and a stiffness of about $4.0 \times 10^8\,\mathrm{N/m^2}$ (tuning frequency of about 800 Hz). As the loss factor is increased beyond 0.3, the noise reduction increases, but only slightly. It is also observed that the maximum noise reduction occurs at a slightly lower stiffness as loss factor increases. This corresponds to the shift in the decay rate peak, for a given stiffness, towards higher frequencies that is seen in Fig. 4.

Although this analysis indicates that a high loss factor is beneficial, materials with a higher loss factor will have a stiffness that varies more significantly with temperature. This inter-relation between damping and stiffness will be considered in the next sections.

4. Temperature dependence of loss factor and stiffness

It is known that the dynamic properties of the absorber will vary with temperature: the higher the loss factor, the bigger the change in the stiffness over a range of temperatures. If the stiffness varies too much, then, as seen above, the absorber will be less effective at extremes of temperature. Conversely, if the loss factor is too low the effect of the absorber is reduced. The balance between these two effects over the range of temperatures required is now investigated.

It is known from Ref. [11] that, for a general elastomer, the slope of the shear storage modulus G' with log frequency is related to the loss modulus G'' by

$$\frac{\mathrm{d}G'}{\mathrm{d}x} = \frac{2G''}{\pi} \tag{9}$$

where $x = \log_e(f)$ and f is frequency. The loss factor η can be written as

$$\eta = \frac{G''}{G'} \tag{10}$$

Substituting this into Eq. (9) gives

$$\frac{dG'}{dx} = \left(\frac{2\eta}{\pi}\right) G' \tag{11}$$

Although the loss factor is generally dependent on frequency and temperature, insight can be gained by assuming a constant value for η. In this case, the solution to Eq. (11) is

$$G' = G_0 e^{((2\eta x)/\pi)} = G_0 f^{(2\eta/\pi)} \tag{12}$$

Thus the ratio of G' at two frequencies f_1 and f_2 is

$$\frac{G'(f_2)}{G'(f_1)} = \left(\frac{f_2}{f_1}\right)^{2\eta/\pi} \tag{13}$$

This frequency-dependence is next converted into a temperature-dependence. According to the principle of time-temperature superposition [12], it is possible to superimpose the curves of G' against $\log_{10} f$ at different temperatures T by adding a temperature-dependent factor $\log_{10} \alpha(T)$ called a shift factor, to $\log_{10} f$. This applies strictly only for a thermorheologically simple material. The shift factor should then be the same for all frequencies for a curve measured at a given temperature.

Thus if $\alpha(T_0) = 1$ at a reference temperature T_0

$$G'(f_1, T_1) = G'(f_2, T_2) = G'(f_0, T_0) \tag{14}$$

where $f_1 = \alpha(T_1) f_0$ and $f_2 = \alpha(T_2) f_0$ are shifted frequencies for temperatures T_1 and T_2. Hence

$$G'(f, T_1) = G'\left(\frac{f}{\alpha(T_1)}, T_0\right) \tag{15}$$

and similarly for T_2, giving

$$\frac{G'(f, T_1)}{G'(f, T_2)} = \frac{G'\left(\frac{f}{\alpha(T_1)}, T_0\right)}{G'\left(\frac{f}{\alpha(T_2)}, T_0\right)} = \left(\frac{\alpha(T_2)}{\alpha(T_1)}\right)^{2\eta/\pi} \tag{16}$$

The Williams–Landel–Ferry (WLF) model [13] can be used to generate a suitable approximation for the factor $\alpha(T)$. This model is found to apply to a wide range of elastomeric materials [12,13]. The WLF model predicts the shift factor as

$$\log_{10} \alpha(T) = \frac{-8.86(T - T_s)}{101.6 + T - T_s} \tag{17}$$

where T_s is a reference temperature applying to a given material. It can be estimated approximately as $T_g + 50$, where T_g is the glass transition temperature of the material [13]. Eq. (17) is valid over a range $T_s - 50 < T < T_s + 50$.

Fig. 8 shows the shift factor for different T_s predicted according to Eq. (17) for temperatures between -20 and 40 °C. These have been normalised by dividing $\alpha(T)$ by the shift factor at 10 °C. The slopes of these curves increase with increasing T_s and decreasing temperature. Using this with Eq. (13), the ratio of storage modulus at two temperatures T_1 and T_2 and for a given frequency is given by

$$\log_{10}\left(\frac{G'(T_1)}{G'(T_2)}\right) = \frac{2\eta}{\pi}\left(\frac{8.86(T_2 - T_s)}{101.6 + T_2 - T_s} - \frac{8.86(T_1 - T_s)}{101.6 + T_1 - T_s}\right) \tag{18}$$

It is now necessary to select a value of T_s. Taking, for example, a value of T_g of -70 °C, corresponding to butyl rubber, T_s will be about -20 °C. Fig. 9 shows the variation of G' with temperature for various loss factors for a value of T_s of -20 °C. The slope of G' increases as the loss factor increases. Here, the value of G' is shown relative to the value at 10 °C.

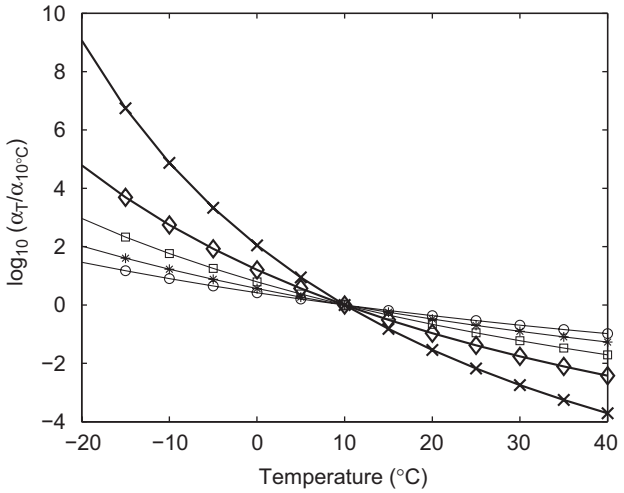

Fig. 8. Logarithm of reduction factor α_T normalised at 10 °C plotted against temperature for various values of T_s. The curves represent ○, $T_s = -40$ °C; ∗, $T_s = -20$ °C; □, $T_s = 0$ °C; ◇, $T_s = 20$ °C; ×, $T_s = 40$ °C.

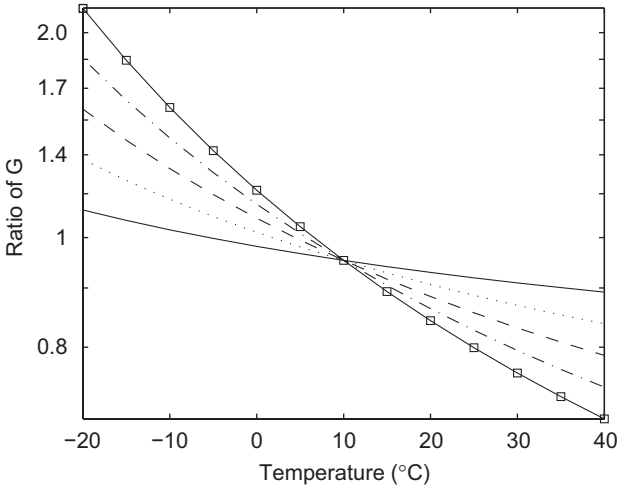

Fig. 9. The ratio of G plotted against temperature for a T_s of −20 °C for temperature normalisation at 10 °C. The curves represent —, $\eta = 0.05$; ⋯, $\eta = 0.1$; − − −, $\eta = 0.2$; − · −, $\eta = 0.4$; □, $\eta = 0.8$.

5. Effect of temperature dependence on noise reduction

If a constant loss factor is assumed, the temperature variation of the stiffness can be introduced into the noise predictions, based on the results of the previous section. Dynamic properties at 10 °C are used as nominal input parameters in the prediction of noise reduction. These are based on a stiffness of 4.36×10^8 N/m^2, corresponding to a tuning frequency of 800 Hz. The stiffness is then varied according to the ratio in Eq. (18), i.e. as given in Fig. 9, as temperature varies and according to Eq. (13) as frequency varies.

Fig. 10 shows the reduction of the vertical rail noise as a contour plot against temperature and damping loss factor. Results are shown for three values of T_s. In all cases, low loss factors give less noise reduction but these results are less sensitive to the change of temperature than at high loss factors. For example, for $T_s = -20$ °C (Fig. 10(b)), a loss factor of 0.1 enables a noise reduction of 3.5 dB to be sustained across most of the temperature range. A loss factor of 0.3 allows a maximum reduction of 5 dB to be achieved and this remains above 4 dB between −10 and 40 °C. However, when the loss factor is increased to 1.0, although the maximum noise reduction is still 5.5 dB, the results are much more strongly dependent on temperature due to the higher

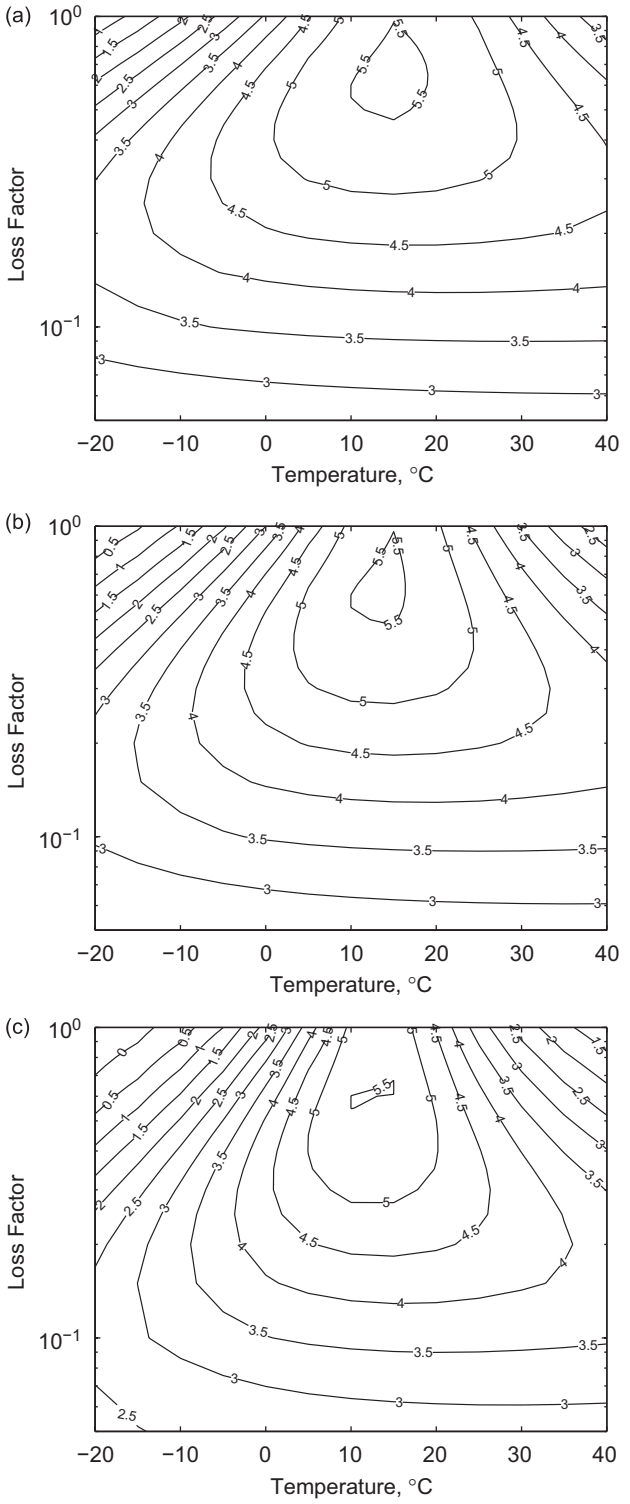

Fig. 10. The reduction of vertical rail noise at various temperatures and loss factors. The parameters used are as in Table 1 with $s_a = 4.36 \times 10^8\ \mathrm{N/m^2}$ at 10 °C. (a) $T_s = -40\,^{\circ}\mathrm{C}$, (b) $T_s = -20\,^{\circ}\mathrm{C}$ and (c) $T_s = 0\,^{\circ}\mathrm{C}$.

variation in stiffness. Generally, a loss factor around 0.25–0.4 appears to give the best results across the range of temperatures considered.

The assumed value of T_s also affects the results. The lowest value of T_s ($-40\,^{\circ}$C) gives less variation of noise reduction across the temperature range than a T_s of $0\,^{\circ}$C. This follows from the stiffness variation seen in Fig. 7. The choice of T_s in the analysis is somewhat arbitrary, but $-20\,^{\circ}$C is realistic for a common workable material such as butyl rubber.

6. Estimating the weighted noise reduction for a range of rail temperatures

Due to the variability of weather and climate the rail temperature varies considerably in the course of a year. This will also have an effect on the performance of the rail absorber. To cover a wide range of situations in Europe, temperature distributions from three different countries, the United Kingdom (UK), Sweden and Italy, have been evaluated. In this section the statistical distribution of rail temperatures is investigated and used to develop a method to estimate a weighted noise reduction based on the rail temperature distribution for any location. This method will be used to assess various elastomeric materials in order to determine the optimum material for any given situation.

Rail and air temperature data were collected at 10 min intervals over a 12 month period [14] at a site at Leominster in the UK and the raw data has kindly been supplied to us by the author. The rail and air temperatures are arranged into a frequency distribution with a $5\,^{\circ}$C resolution. In Fig. 11 the distribution of rail temperature can be used as a weighting for the noise reduction obtained at each temperature. Thus most account should be taken of the noise reduction at $10\,^{\circ}$C, and relatively little of that at -10 and $40\,^{\circ}$C. The distribution of air temperatures is similar to that of the rail at low temperatures, but the rail temperature has more occurrence at high temperatures because of the effect of sunlight.

To gain an impression of the likely distribution of rail temperatures in other countries, use has been made of more widely available meteorological data in the form of daily maximum and minimum air temperatures. For Sweden, data were obtained for Fulum covering the period from January to December 2000 and for Italy were obtained for Brindisi from January to December 2005 [15].

Figs. 12(a) and (b) show distributions of the maximum and minimum daily air temperature for Sweden and Italy, again in $5\,^{\circ}$C intervals. At the location in Italy, the temperature range is 0–$35\,^{\circ}$C. The distributions of minimum and maximum temperature are similar apart from a constant shift. For Sweden the temperature distributions contain a large 'tail' at low temperatures. The range of temperatures here is between -30 and $25\,^{\circ}$C.

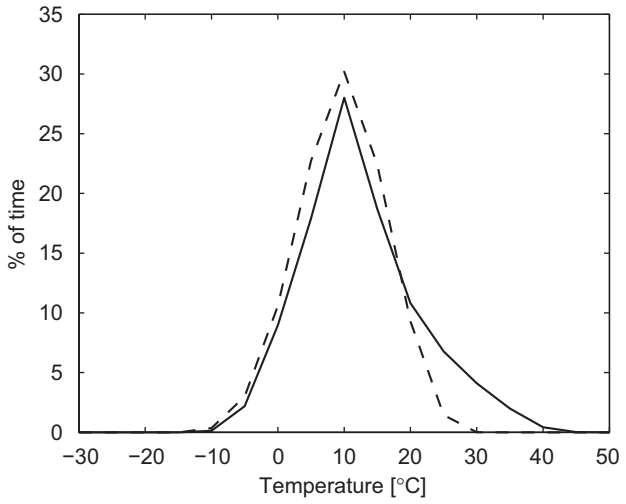

Fig. 11. Distribution of rail temperature (—) and instantaneous air temperature (– –) throughout the year for Leominster, UK.

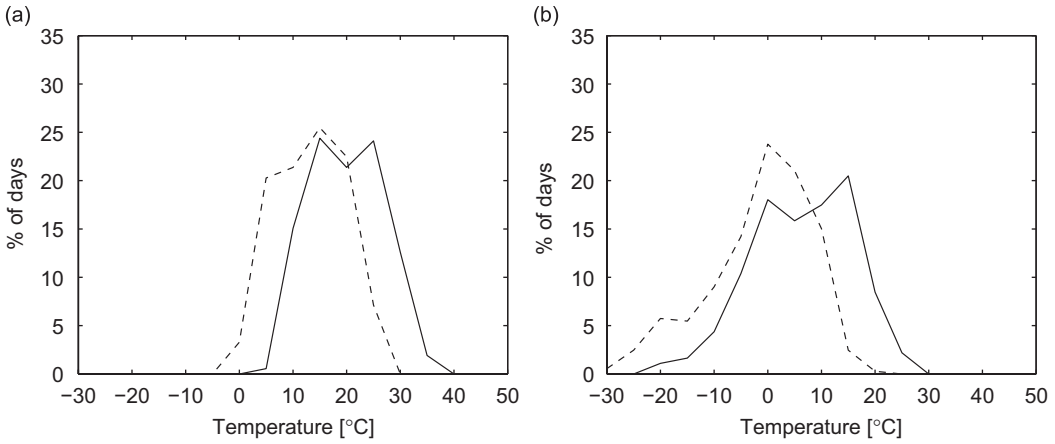

Fig. 12. Maximum (—) and minimum (−−) daily temperature throughout the year for (a) Italy and (b) Sweden.

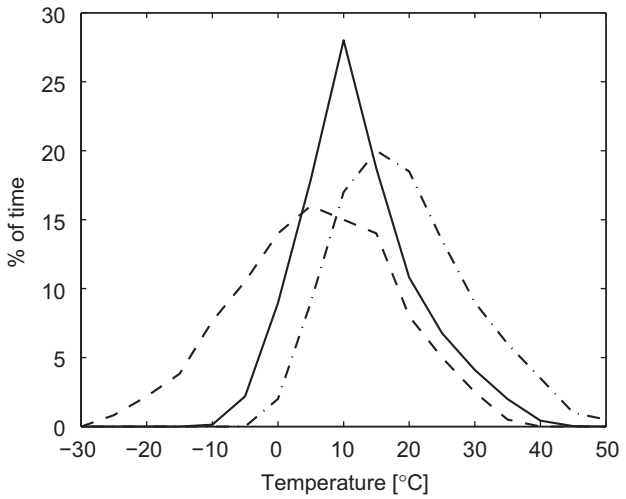

Fig. 13. Rail temperature distribution for UK (—) and estimated for Sweden (−−) and Italy (− · −).

As the temperature data from Sweden and Italy do not include rail temperature, the rail temperature distribution obtained from the UK site has been used as a guide to estimate the rail temperature distribution for Sweden and Italy. To do that, it is convenient to take the points mid-way between the maximum and minimum air temperature for each day of the year. The data from the UK site has been converted to this form so that comparisons can be made.

Based on these distributions, plausible rail temperature distributions that are consistent with the available air temperatures have been determined. The results of the estimation are shown in Fig. 13. The rail temperature for the UK is in the range −10 to 40 °C, Italy in the range 0–50 °C and Sweden in the range −25 to 35 °C.

The temperature distributions in Fig. 13 can be used as weighting functions. A temperature-weighted noise reduction for each country can be estimated based on these. The weighted noise reductions have been determined as follows. For a given loss factor and stiffness at 10 °C (which can also be expressed in terms of the tuning frequency at 10 °C), the corresponding stiffnesses are determined at each temperature in the range −20 to 40 °C. For each of these temperatures the rail decay rate is determined and used to find the noise

reduction achieved by the absorber. The results for each temperature are then weighted using the factors shown in Fig. 13 to give a weighted noise reduction.

$$\Delta L_{A,T} = \sum_{i=1}^{n} (w_{T,i} \times \Delta L_{A,i}) \tag{19}$$

where $\Delta L_{A,T}$ is the average weighted noise reduction with respect to temperature, $w_{T,i}$ is the weighting factor for temperature i and $\Delta L_{A,i}$ is the A-weighted noise reduction for temperature i.

Fig. 14 shows the results using the UK weighting for a range of loss factors and stiffnesses. This shows that the maximum benefit is found for a nominal tuning frequency of 800 Hz at 10 °C and loss factors between 0.25 and 0.75. Fig. 14(b) confirms this by showing the results for the nominal tuning frequency of 800 Hz plotted against loss factor.

Fig. 15 shows the equivalent results for the Swedish weighting. Fig. 15(a) shows that the greatest weighted noise reduction occurs for a tuning frequency of about 700 Hz at 10 °C. As this material gets stiffer at lower temperatures, this will mean that the tuning frequency will be around 800 Hz for the most common temperature of 5 °C. The maximum benefit is slightly reduced due to the wider spread of temperatures, particularly low temperatures, included in the weighting. The result in Fig. 15(b) falls more rapidly at high loss factors than for the UK weighting.

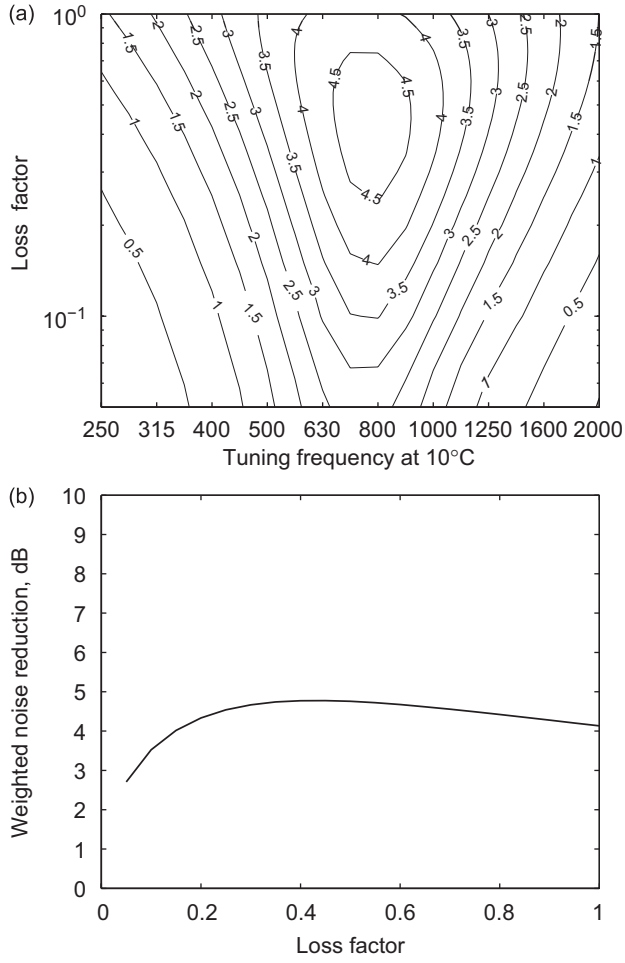

Fig. 14. (a) Contour plots of weighted noise reduction against tuning frequencies and loss factor for UK weighting. (b) The effect of various loss factors on the weighted noise reduction for tuning frequencies at 10 °C of 800 Hz.

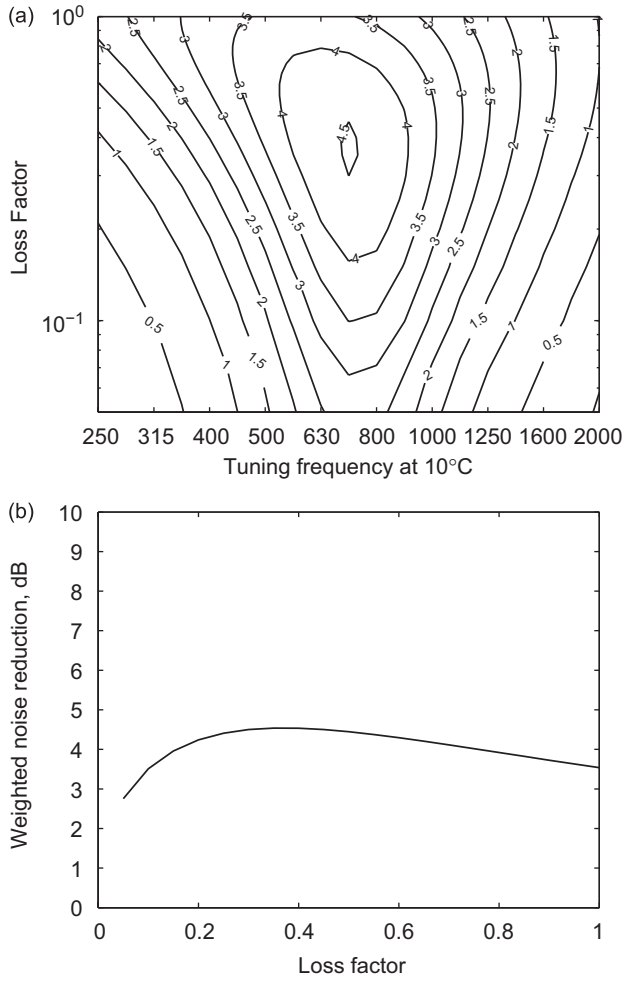

Fig. 15. (a) Contour plots of weighted noise reduction against tuning frequencies and loss factors for Swedish weighting. (b) The effect of various loss factors on the weighted noise reduction for tuning frequency at 10 °C of 700 Hz.

Fig. 16 shows the weighted noise reduction for Italy. This shows the opposite trend, with the maximum benefit for a slightly stiffer material, which gives a tuning frequency of 800 Hz at 15 °C. The maximum benefit and dependence on loss factor are similar to the results for the UK.

7. Conclusions

An investigation has been made into the optimum damping loss factor and stiffness of the elastomer in a rail absorber, in terms of the reduction of noise that can be achieved. In order to calculate the noise reduction, a mathematical model of a beam was used to represent the rail. The noise reduction from the vertical wave is most important and the rail absorber has to be optimised for this component.

The reduction of noise is influenced by changes of temperature. Knowing that the stiffness is very sensitive to temperature, an approximate technique has been adopted to estimate this effect. By assuming a constant loss factor, the variation in stiffness across the temperature range has been estimated, assuming only a value for the temperature T_s as used in the WLF equation. It is shown that the noise reduction can be maintained within 1 dB of the maximum effect in a range −10 to 40 °C for a loss factor of about 0.3. With lower loss factors the result is less sensitive to temperature but the overall reduction obtained is smaller. With higher loss

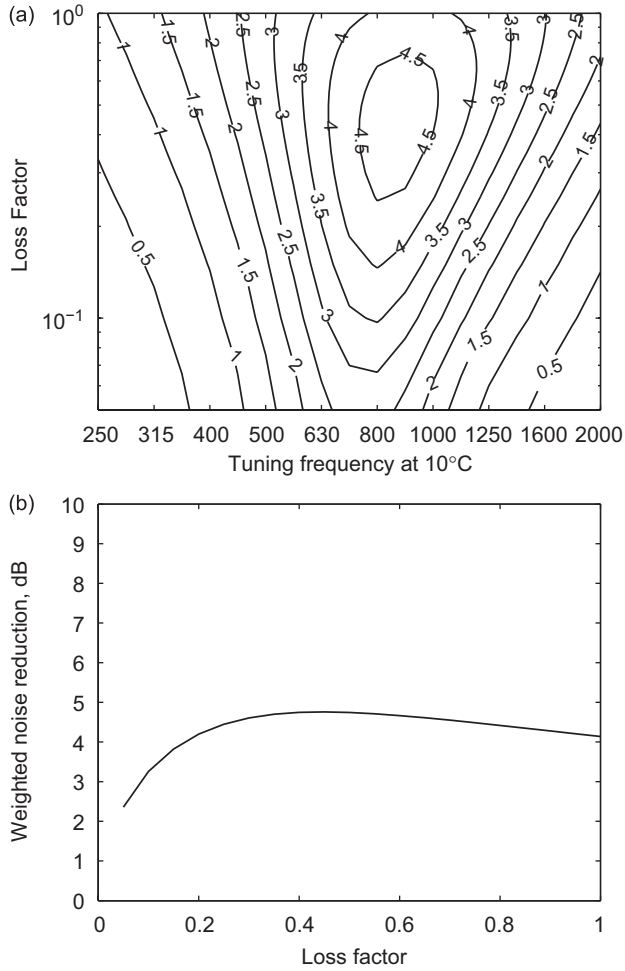

Fig. 16. (a) Contour plots of noise reduction against tuning frequencies and loss factor for Italian weighting. (b) The effect of various loss factors on the weighted noise reduction for tuning frequencies at 10 °C of 900 Hz.

factors, although the same maximum reduction can be achieved, this is much more sensitive to variations in temperature.

Rail temperature distributions can be used as weighting functions for the noise reduction to ensure that a rail absorber design is focussed on the temperatures that occur most commonly at a given location. For the UK, the most common temperature is at 10 °C so the maximum noise reduction is required at this temperature. For Italy a slightly stiffer material is required to give the maximum noise reduction at around 15 °C, while for Sweden a slightly softer material is required.

The analysis method presented here could be readily extended to study more complex absorber designs accounting for the temperature- and frequency-dependence of real elastomers but that is beyond the scope of the present paper.

References

[1] D.J. Thompson, C.J.C. Jones, A review of the modelling of wheel/rail noise generation, *Journal of Sound and Vibration* 231 (2000) 519–536.

[2] D.J. Thompson, P. Fodiman, H. Mahé, Experimental validation of the TWINS prediction program for rolling noise, part 2: results, *Journal of Sound and Vibration* 193 (1) (1996) 137–147.

[3] J. Oertli, The STAIRRS project, work package 1: a cost-effectiveness analysis of railway noise reduction on a European scale, *Journal of Sound and Vibration* 267 (2003) 431–437.
[4] D.J. Thompson, C.J.C. Jones, T.P. Waters, D. Farrington, Tuned damping device for reducing noise from railway track, *Applied Acoustics* 68 (2007) 3–57.
[5] A.D. Nashif, D.I.G. Jones, J.P. Henderson, *Vibration Damping*, Wiley, New York, 1985.
[6] C.J.C. Jones, D.J. Thompson, R.J. Diehl, The use of decay rates to analyse the performance of railway track in rolling noise generation, *Journal of Sound and Vibration* 293 (2006) 485–495.
[7] D.J. Thompson, A continuous damped vibration absorber to reduce broad-band wave propagation in beams, *Journal of Sound and Vibration* 311 (3–5) (2008) 824–842.
[8] K.F. Graff, *Wave Motion in Elastic Solids*, Dover, New York, 1997.
[9] S.L. Grassie, R.W. Gregory, D. Harrison, K.L. Johnson, The dynamic response of railway track to high frequency vertical excitation, *Journal of Mechanical Engineering Science* 24 (1982) 77–90.
[10] D.J. Thompson, B. Hemsworth, N. Vincent, Experimental validation of the TWINS prediction program for rolling noise, part 1: description of the model and method, *Journal of Sound and Vibration* 193 (1) (1996) 123–135.
[11] F.R. Schwarzl, L.C.E. Struik, Analysis of relaxation measurement, *Advance in Molecular Relaxation Processes* 1 (3) (1968) 201–255.
[12] J.D. Ferry, *Properties of Polymers*, second ed., Wiley, New York, 1970.
[13] J.D. Williams, R.F. Landel, J.D. Ferry, The temperature dependence of relaxation mechanisms in amorphous polymers and other glass-forming liquids, *Journal of the American Chemistry Society* 77 (1955) 3701–3707.
[14] L. Chapman, J.E. Thornes, Y. Huang, X. Cai, V.L. Sanderson, S.P. White, Modelling of rail surface temperatures: a preliminary study, *Theoretical and Applied Climatology* 92 (2008) 121–131.
[15] European Climate Assessment and Data, Temperature distribution ⟨www.eca.knmi.nl⟩, accessed August 25, 2007.